

Open Access

Survival, Exercise Capacity, and Left Ventricular Remodeling in a Rat Model of Chronic Mitral Regurgitation: Serial Echocardiography and Pressure-Volume Analysis

Kyung-Hee Kim, MD, Yong-Jin Kim, MD, Seung-Pyo Lee, MD, Hyung-Kwan Kim, MD, Jeong-Wook Seo, MD, Dae-Won Sohn, MD, Byung-Hee Oh, MD, and Young-Bae Park, MD

Department of Internal Medicine, Cardiovascular Center, Seoul National University College of Medicine, Seoul, Korea

ABSTRACT

Background and Objectives: The aims of this study were to establish a reliable model of chronic mitral regurgitation (MR) in rats and verify the pathophysiological features of this model by evaluating cardiac function using serial echocardiography and a pressure-volume analysis. **Materials and Methods :** MR was created in 37 Sprague-Dawley rats by making a hole with a 23 gauge needle on the mitral leaflet through the left ventricular (LV) apex under the guidance of transesophageal echocardiography. **Results:** Serial echocardiograms revealed that the LV began to dilate immediately after the MR operation and showed progressive dilation until the 14th week (LV end-systolic dimension at 14 weeks, 4.71 ± 0.25 mm vs. 6.81 ± 0.50 mm for sham vs. MR, $p < 0.01$; LV end-diastolic dimension, 8.32 ± 0.42 mm vs. 11.01 ± 0.47 mm, $p < 0.01$). The LV ejection fraction tended to increase immediately after the MR operation but started to decrease thereafter and showed a significant difference with the sham group from the 14th week ($70.0 \pm 2.2\%$ vs. $62.1 \pm 3.1\%$ for sham vs. MR). In a pressure-volume analysis performed at the 14th week, the LV end-systolic pressure-volume relationship and $+dp/dt$ decreased significantly in the MR group. A serial treadmill test revealed that exercise capacity remained in the normal range until the 14th week when it began to decrease (exercise duration, 406 ± 45 seconds vs. 330 ± 27 seconds, $p < 0.01$). A pathological analysis showed no significance difference in interstitial fibrosis between the two groups. **Conclusion:** We established a small animal model of chronic MR and verified its pathophysiological features. This model may provide a useful tool for future research on MR and volume overload heart failure. (*Korean Circ J* 2011;41:603-611)

KEY WORDS: Mitral regurgitation; Hemodynamic study; Exercise test; Rat model.

Introduction

Heart failure is a leading cause of death and continues to provide significant socioeconomic burdens worldwide.¹⁾ Heart failure is a clinical syndrome attributed to various causes. Although most patients share the final stage of left ventricular

(LV) dysfunction, the pathophysiology from initial myocardial damage to LV dysfunction differs in every patient.²⁾ Therefore, the study of heart failure requires various animal models that mimic the pathogenetic features of heart failure in humans. In this respect, rat models of LV hypertrophy that lead to heart failure have been useful for examining pathogenesis and for testing novel heart failure therapeutic options.³⁾⁴⁾ Many investigators have scaled down from large animal models to rat models because they are easier to manipulate, cheaper to maintain, and similar to the human cardiovascular system. Moreover, recent advances in echocardiography and micromanometer conductance catheters have made it possible to reliably evaluate cardiac function in rats.⁵⁾

Mitral regurgitation (MR) is the most common type of valvular heart disease that induces LV volume overload. The prevalence of MR has been increasing as the mean age of the population advances.⁶⁾⁷⁾ However, the pathophysiology of MR

Received: May 17, 2011

Revision Received: June 24, 2011

Accepted: June 27, 2011

Correspondence: Yong-Jin Kim, MD, Department of Internal Medicine, Seoul National University College of Medicine, Cardiovascular Center, 101 Daehak-ro, Jongno-gu, Seoul 110-744, Korea
Tel: 82-2-2072-1963, Fax: 82-2-2072-2577
E-mail: kimdamas@snu.ac.kr

• The authors have no financial conflicts of interest.

© This is an Open Access article distributed under the terms of the Creative Commons Attribution Non-Commercial License (<http://creativecommons.org/licenses/by-nc/3.0>) which permits unrestricted non-commercial use, distribution, and reproduction in any medium, provided the original work is properly cited.

has not been fully understood partly because adequate animal models are not yet available. Although large animal models (dog or sheep)⁸⁾⁹⁾ have been used, they are limited because of the small sample sizes of the experimental groups. In the present study, we established a reliable small animal model of chronic MR using rats and verified the pathophysiological features of this model by evaluating cardiac function using serial echocardiography and pressure-volume (PV) analysis to provide a useful tool for future research on cardiac remodeling in MR and volume-overload heart failure.

Materials and Methods

In total, 61 Sprague-Dawley (SD) rats (initial weight, 350-400 g) were used at the age of 10 weeks. The rats were given access to tap water and standard rat chow ad libitum and were housed in the Laboratory Animal Facility of the Clinical Research Institute of Seoul National University Hospital with a 12 hours :12 hours light cycle and a temperature of 21°C. The experimental protocols were approved by the Institutional Animal Care and Use Committee of Seoul National University Hospital.

Creation of mitral regurgitation

Mitral regurgitation was created in 37 of 61 rats 1 week after baseline echocardiography, the exercise test, and blood pressure (BP) measurements, as previously described.¹¹⁾ The rats were anesthetized with 3% isoflurane at a rate of 4 L/min oxygen and were intubated with a blunt 16-gauge needle, followed by mechanical ventilation with an M-683 system (Harvard Apparatus Inc., Holliston, MA, USA) under 2-3% isoflurane in a mixture of 50% O₂. Body temperature was maintained at 37°C by placing the rats on a heating pad during the procedure. After successful anesthesia, an intracardiac echocardiographic catheter (AcuNav™, Acuson/Siemens Corp, Mountain View, CA, USA) was inserted into the esophagus for transesophageal echocardiography. A lateral thoracotomy was performed, and the pericardium was opened. The LV was gently pressed with a clean cotton swab to accurately locate the insertion site of the puncture needle. A needle (23 gauge, 0.5 mm external diameter) was inserted into the LV via apical puncture and was advanced toward the mitral valve to create a hole in the leaflet and induce MR under the guidance of transesophageal echocardiography (Fig. 1). MR was considered significant if a regurgitant jet area occupied >45% of the left atrium (LA).¹⁰⁾ The sham group (n=24) underwent the same

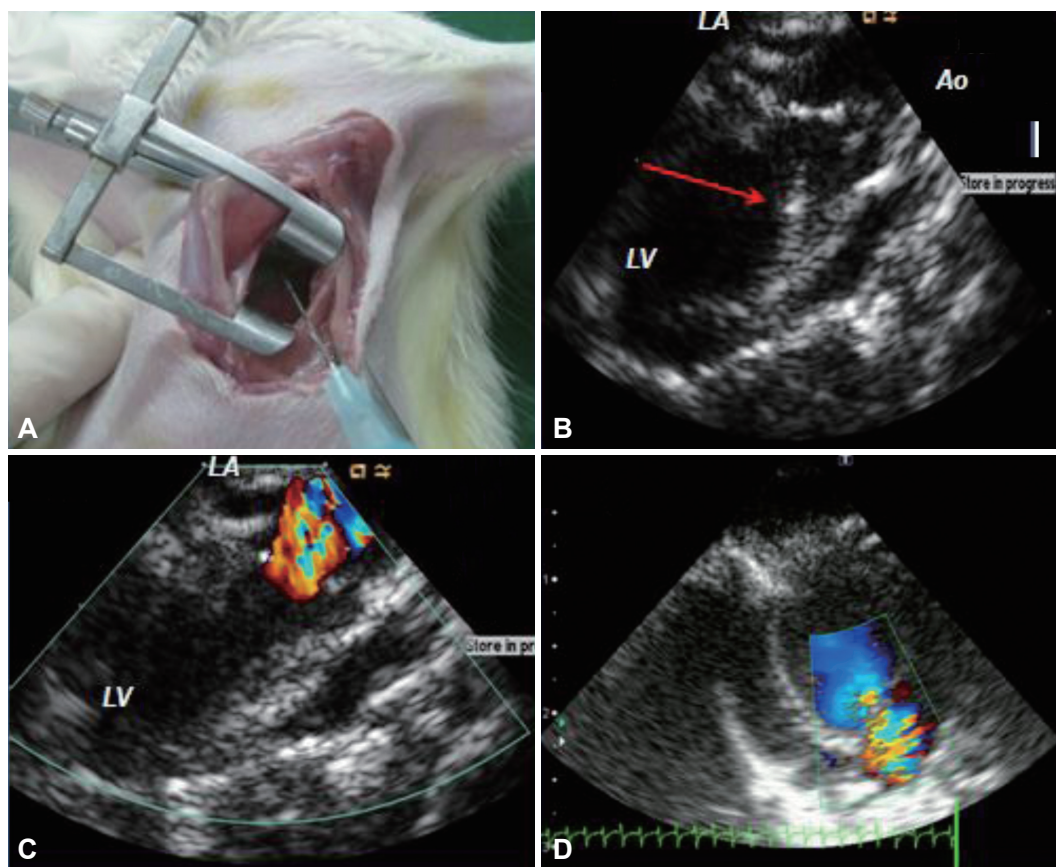


Fig. 1. Surgical procedures for creating mitral regurgitation (MR). A: a lateral thoracotomy was performed on the left side of the sternum through the 3rd or 4th intercostal space, and a needle was inserted. B: advancing the needle toward the mitral valve leaflet; red arrow indicates the needle. C: severe MR events were detected by color Doppler after the MR procedure. D: the MR jet and left atrial area were measured 1 week after MR development by transthoracic echocardiography.

procedure but without damage to the mitral valve. All rats were given a 2 mL subcutaneous injection of isotonic saline and meloxicam (Boehringer Ingelheim, Germany 0.4 mg/g s.c.) postoperatively and cefazolin (50 µg/g i.m.) 2 times per day for 2 days to prevent infection.

Echocardiography

Transthoracic echocardiography was performed 1 week before and 1, 3, 6, 9, 12, and 14 weeks after the creation of MR on spontaneously breathing rats placed in a dorsal recumbent position. Rats were lightly sedated with the lowest possible dose of isoflurane (initially 4%, then approximately 2-3%) mixed with oxygen. Images were acquired with a 9 MHz transducer connected to a Toshiba echocardiography machine (Nemio, Toshiba Co., Tokyo, Japan). LV septal and posterior wall thickness (SWT and PWT, respectively) and the LV end diastolic/systolic dimension (EDD/ESD, respectively) were measured using M-mode echocardiography at the papillary muscle level. The LV ejection fraction (EF) was calculated as $(LVEDD^2 - LVESD^2) / LVEDD^2$. LV mass was estimated by a formula previously validated in small animals^{11,12} and adjusted for body weight: $[LV\text{-mass} = \{(SWT + PWT + LVEDD)^3 - (LVEDD)^3\} \times 1.04]$. Color Doppler mapping of MR jets was used to semiquantitatively assess the severity of MR.¹³ MR jet and LA areas were measured in the apical long-axis view, and the ratio of MR jet area to the LA areas was calculated (Fig. 1D). Early diastolic transmitral flow (E velocity) was measured in an apical four-chamber view with a 1.5-mm sized sample volume placed at the tips of the mitral leaflets. Early diastolic septal mitral annulus velocity (E') was assessed by tissue Doppler imaging with a sample volume of 1 mm. All parameters were evaluated on an average of five consecutive beats. A single echocardiographer, with >500 rat echocardiography cases of experience, performed all data acquisition.

Exercise test and blood pressure monitoring

Maximal exercise capacity was evaluated with the Rota Rod Treadmill (Ugo Basile, Comerio, Italy). The rats ran on a knurled drum as the drum rotated to avoid falling off. Animals were trained two times before the test to adjust the treadmill. Treadmill speed was gradually increased from 3 revolutions per minute (rpm) to 15 rpm every 1 minute, and maximum exercise time was recorded. An observer blinded to the study group recorded the immobility response due to exhaustion.

Systolic and diastolic BPs were measured in conscious rats using the tail-cuff method (Biopac System Inc., Goleta, CA, USA) at 10, 14, 18, and 22 weeks of age. At minimum of 1 day was given for the BP measurements after the echocardiographic examination or exercise test to minimize stress on the animals.

Hemodynamic measurements

At 14 weeks after MR creation, the rats were anesthetized

with isoflurane and placed in the supine position on a heating pad with a rectal probe connected to a thermoregulator. The right internal jugular vein was cannulated to administer fluids. After an anterior thoracotomy, a microtip PV catheter (SPR-838, Millar Instruments, Houston, TX, USA) was introduced into the LV cavity via an apical approach along the longitudinal axis of the heart until stable PV loops were obtained.^{5,14} PV loops were acquired with the ventilator off for 5-10 seconds after 10 minutes of stabilization. The sampling rate was 1,000/s using the ARIA PV conductance system (Millar Instruments) coupled to a PowerLab/4SP A/D converter (AD Instruments; Mountain View, CA, USA) and a personal computer. To obtain V_o , additional loops were acquired during injection of 500 µL of 15% hypertonic saline. Ten to twenty successive cardiac cycles were obtained. True corrected volumes were calculated based on the EF on echocardiography and saline calibrations, as described previously.^{5,15} Analyses of the loops were performed using a commercially available cardiac PV analysis program, PVAN 3.5 (Millar Instruments).

Heart rate, maximal LV systolic pressure, LV end-diastolic pressure (EDP), mean arterial pressure, maximal slope of systolic pressure increment (+dP/dt), the decrease in diastolic pressure (-dP/dt), the time constant of LV pressure decay (τ), stroke volume (SV), and end-systolic/diastolic volume (ESV/EDV) were calculated. Additionally, the end-systolic pressure volume relationship (ESPVR), the SW-EDV relationship {pre-load recruitable stroke work (PRSW)}, the dP/dt_{max}-EDV relationship, and the end-diastolic PV relationship (EDPVR) were measured by transient occlusion of the inferior vena cava with a silk snare suture.¹⁶

Survival assessment

The survival analysis was performed for animals that survived the acute stage of MR (2 weeks after the surgical procedure) until 14 weeks after MR when a hemodynamic study was performed. Ten rats from each group were randomly chosen and followed up for 10 months to evaluate long-term survival.

Histological analysis

After the hemodynamic measurements, the rats were euthanized and the hearts and lungs were harvested. Hearts and lungs were dissected after they were rinsed with isotonic saline and weighed. The weights of the hearts and lungs were normalized to body weight and used as an index of ventricular hypertrophy and pulmonary congestion, respectively. The LV was then fixed with 4% paraformaldehyde and embedded in paraffin. The tissue was sectioned into 4 µm sections, stained with Masson's trichrome to evaluate the degree of fibrosis and with picosirius red to measure collagen deposition. The measurement of the area of fibrosis was quantified as the ratio of the area of fibrosis surrounding the total myocardium area using NIH image analysis software (Image J ver.

1.38, National Institutes of Health).¹⁷⁾ An arterial blood sample was collected from the abdominal aorta immediately after the hemodynamic measurements. After centrifugation (3,000×g), the plasma was stored at -80°C and assayed for plasma brain natriuretic peptide (BNP). BNP concentration was assessed with a rat ELISA rat BNP-45 kit (Assaypro, St. Charles, MO, USA).

Statistical analysis

The results are expressed as means±SD. The unpaired two-sided Student's t-test was used to compare continuous variables between groups, as appropriate. The time course of parameter changes was compared between the sham and MR groups using a repeated-measures analysis of variance. Survival rate was evaluated by the Kaplan-Meier method. All statistical analyses were performed using SPSS version 17.0 (SPSS Inc., Chicago, IL, USA), and $p < 0.05$ were considered statistically significant.

Results

Two rats died of bleeding and one rat died of an unknown cause after surgery, making the operative mortality 8% (3/37). Four rats died during the acute stage within 2 weeks after the MR operation (12%, 4/34) due to pulmonary edema (3/4) and an unknown cause (1/4). No death was noted in the sham group. Two weeks after surgery, 54 rats (24 in the sham group and 30 in the MR group) remained alive for the study. The mean weight gain of the MR rats during the 14 week period tended to lag behind the sham rats, but no statistical difference was observed (Fig. 2A)

Mitral regurgitation severity and Doppler echocardiographic data (Table 1)

Mitral regurgitation was created successfully in all rats. Mean MR jet area was $15 \pm 3 \text{ mm}^2$, and the mean ratio of MR jet area to LA area was $56 \pm 8\%$ at 1 week. No MR occurred in the

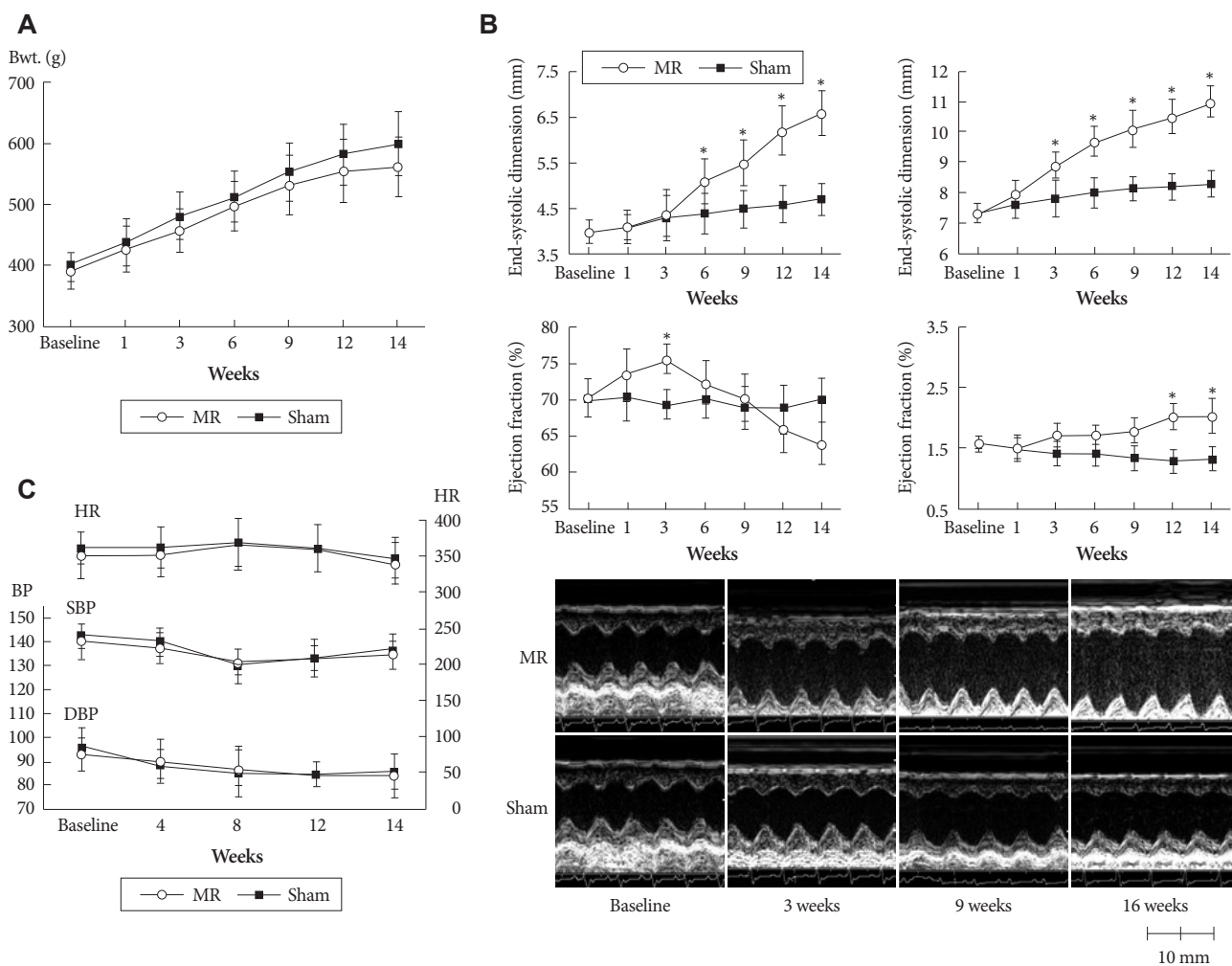


Fig. 2. Left ventricular remodeling after mitral regurgitation. A: body weight changes between the mitral regurgitation (MR) and the sham group. B: serial changes in cardiac remodeling using echocardiographic measurements. Time course of typical M-mode echocardiograms. End-systolic dimension (mm), end-diastolic dimension (mm), left ventricular (LV) ejection fraction (%), LV mass index, g/kg. * $p < 0.05$. C: serial changes in blood pressure and heart rate. MR: mitral regurgitation, LV: left ventricular, LVPWT: left ventricular posterior wall thickness, HR: heart rate, SBP: systolic blood pressure, DBP: diastolic blood pressure.

sham group. Mitral E velocity increased at 1 week (65.2 ± 7.1 cm/s vs. 105.1 ± 15.1 cm/s, $p < 0.01$) in the MR group, whereas it did not change in the sham group (66.4 ± 6.4 cm/s vs. 64.5 ± 5.5 cm/s, $p = 0.76$). However, E velocity was similar at 6 weeks after MR and throughout the study period. So, the E/E' ratio was not different between the groups at 6 weeks after the operation (Supplementary Fig. 1).

Left ventricular remodeling after mitral regurgitation

Fig. 2B demonstrates the time-dependent changes in LV diameter and the EF and LV mass index. Baseline examinations showed no differences in LV diameters between the two groups (LVESD, 4.02 ± 0.27 mm vs. 4.03 ± 0.24 mm, LVEDD; 7.31 ± 0.34 mm vs. 7.34 ± 0.29 mm for the sham and MR groups, respectively $p = 0.82$). The LV started to dilate immediately after MR and showed progressive dilation until the 14th week. Significant differences in LVEDD were observed between the groups from the 3rd week after MR, whereas LVESD did not increase significantly until the 6th week. LVEF tended to increase immediately after MR, suggesting hyper-

dynamic systolic function but started to decrease thereafter. A significant difference was observed in LVEF between the groups at the 14th week. LV mass index progressively increased in the MR group. No significant changes were observed for BP or heart rate between the groups (Fig. 2C)

Hemodynamic measurements and plasma brain natriuretic peptide level

The 15 MR rats and 14 sham rats underwent an invasive hemodynamic assessment randomly and were sacrificed for the pathological analysis (Table 2). Heart rate, LVEDP, $-dp/dt$, τ (Weiss, Glantz), and the EDPVR slope were not different between the groups. However, ESV, EDV, and SV were gr-

Table 1. Echocardiographic characteristics at 14 weeks after mitral regurgitation (25 weeks of age)

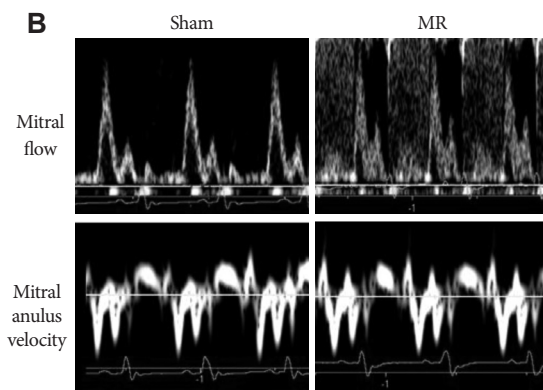
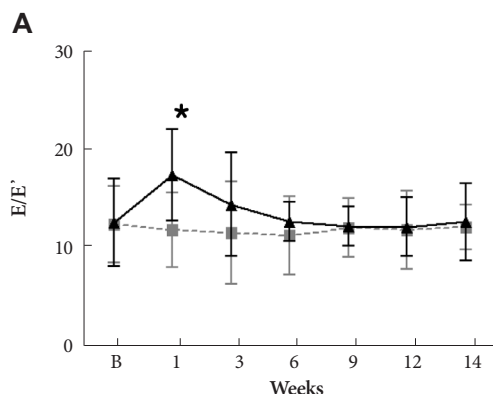
Variables	Sham group (n=24)	MR group (n=25)	P
HR (beats/min)*	312.8±27.3	318.3±15.7	0.84
EF (%)	70.0±2.2	62.1±3.1	<0.01
EDD (mm)	8.32±0.42	11.1±0.47	<0.01
ESD (mm)	4.57±0.25	6.81±0.50	<0.01
SWT (mm)	1.35±0.07	1.30±0.08	0.1
PWT (mm)	1.32±0.08	1.19±0.06	0.04
E/E'	12.0±3.2	12.5±5.5	0.75
LV mass index (mg/g)*	1.31±0.23	2.04±0.29	<0.01

Data are means±SD. *Heart rate and LV mass were estimated *in vivo* by echocardiography. HR: heart rate, EF: ejection fraction, SWT: end-diastolic wall thickness of the interventricular septum, PWT: end diastolic wall thickness of the posterior wall, EDD: end diastolic dimension, ESD: end systolic dimension, E/E': mitral inflow E-septal tissue Doppler velocity E' ratio

Table 2. Hemodynamic parameters

Variables	Sham group (n= 14)	MR group (n=15)	p
HR (beats/min)	315.5±36.3	321.1±24.7	0.27
ESV (μL)	126.2±25.9	390.2±47.4	<0.01
EDV (μL)	403.9±55.6	998.7±134.7	<0.01
EF (%)	69.0±2.8	60.9±3.8	<0.01
SV (μL)	277.7±31.8	608.5±92.3	<0.01
LV ESP (mm Hg)	90.0±14.3	87.5±13.4	0.57
LV EDP (mm Hg)	10.1±3.1	12.0±5.0	0.09
+dP/dt (mm Hg/s)	5951.1±1002.5	4260.8±603.3	0.04
-dP/dt (mm Hg/s)	-3954.7±981.7	-3535.5±585.5	0.31
τ (Weiss) (ms)	20.3±14.5	19.8±4.2	0.84
τ (Glantz) (ms)	14.7±1.2	15.5±4.3	0.61
ESPVR (mm Hg/μL)	0.371±0.153	0.130±0.396	0.02
EDPVR (mm Hg/μL)	0.016±0.006	0.012±0.005	0.32
PRSW (mm Hg)	111.1±24.5	68.7±14.2	0.01
dP/dtmax-EDV (mm Hg/s · μL)	21.26±4.5	8.03±3.4	0.01

Mean±standard deviation. MR: mitral regurgitation group, HR: heart rate, ESV: end-systolic volume, EDV: end-diastolic volume, SV: stroke volume, LV ESP: LV end systolic pressure, LV EDP: LV end diastolic pressure, ESPVR: end systolic pressure-volume relationship, EDPVR: end diastolic pressure-volume relationship



Supplementary Fig. 1. A: serial change in mitral inflow E-septal tissue Doppler velocity E' ratio (E/E'). * $p < 0.05$. B: a representative image at 9 weeks after development of mitral regurgitation.

eater in the MR group than those in the sham group. The ESPVR slope, $+dp/dt$, and EF decreased significantly in the MR group, indicating contractile dysfunction (Fig. 3).

The plasma BNP concentration of the sham rats at the 14th week after MR was below the detection limit (<30 pg/mL). Plasma BNP concentration increased to 105 ± 62 pg/mL in rats with MR.

Exercise capacity

No difference in exercise duration was observed between the groups until the 14th week after MR when exercise duration became shorter in the MR group (406 ± 45 seconds vs. 330 ± 27 seconds, $p < 0.01$) (Fig. 4). Thereafter, exercise capacity was impaired progressively (at 24 weeks, 370 ± 40 seconds vs. 180 ± 14 seconds, $p < 0.01$).

Survival analysis and pathological results

Fig. 5 shows the Kaplan-Meier survival curves in the MR and sham groups. The survival rate at the 14th week after MR was worse in the MR group (83.3%, 25/30) than that in the

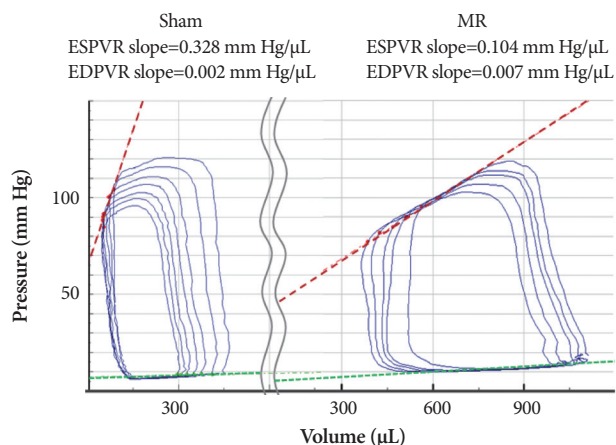


Fig. 3. The mitral regurgitation (MR) model phenotype. Pressure-volume loops depict the features of MR. The slope of the end-systolic pressure volume relation (ESPVR, red slope) is an excellent load-independent index of myocardial contractility. Compared with the sham heart (left) the MR heart is enlarged, and has depressed contractility.

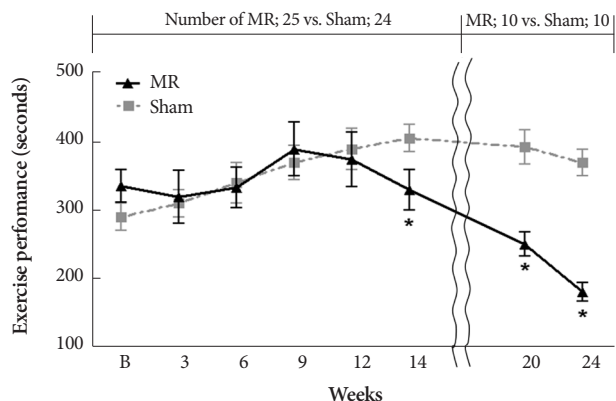


Fig. 4. A comparison of exercise capacity measured by running duration to exhaustion in the two groups during the compensated and decompensated phases. $p < 0.01$.

sham group (100%; 24/24, $p = 0.038$). Among 30 rats with chronic MR and 24 sham rats, 10 rats in each group were randomly followed up for 10 months. The 10-month survival rate was significantly lower in the MR group than that in the sham group (50% for MR vs. 90% for sham; $p < 0.01$).

A gross pathological examination showed that the heart was significantly enlarged in the MR group with eccentric hypertrophy at 14 weeks postoperatively (Table 3) (Fig. 6). However, quantitative measurements of interstitial fibrosis and collagen showed no differences between the groups.

Discussion

A wide variety of small animal heart failure models are available.^{3,18} The role of these models for understanding the disease and developing new treatment cannot be overemphasized. In the present study, we established a small animal MR model in rats and evaluated survival, exercise capacity, and LV remodeling using serial echocardiographic follow-up and a PV analysis. We believe that this model will provide a

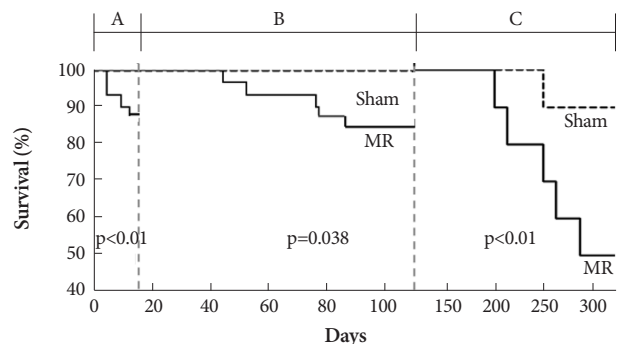


Fig. 5. Landmark analysis of Kaplan-Meier survival rate in rats with and without mitral regurgitation (MR). A phase; four rats died due to pulmonary edema during the acute stage within 2 weeks after the MR operation (12%, 4/34). All sham-operated rats ($n = 24$) were alive. B phase; the survival rate during the chronic compensated stage tended to be worse in the MR group (83.3%, 25/30) than that in the sham group (100%; 24/24, $p = 0.038$). C phase; ten rats in each group were followed up for 10 months. The 10 month survival rate was significantly lower in the MR group than that in the sham group (50% for MR vs. 90% for sham).

Table 3. Pathology results

Variables	Sham group (n = 14)	MR group (n = 15)	P
BW (g)	598.0 \pm 52.0	561.0 \pm 48.8	0.34
Heart (g)	1.16 \pm 0.11	1.52 \pm 0.45	0.02
Lung (g)	1.66 \pm 0.15	1.81 \pm 0.20	0.04
Liver (g)	19.7 \pm 2.5	18.2 \pm 1.95	0.66
Heart/BW (mg/g)	1.94 \pm 0.34	2.71 \pm 0.62	<0.01
Lung/BW (mg/g)	2.81 \pm 0.29	3.23 \pm 0.31	0.01
Liver/BW (mg/g)	33.1 \pm 2.9	32.5 \pm 3.5	0.76
Interstitial fibrosis (%)	4.9 \pm 2.6	5.0 \pm 3.1	0.88
Interstitial collagen (%)	3.7 \pm 1.7	3.7 \pm 2.1	0.90

Values are means \pm SDs. BW: body weight

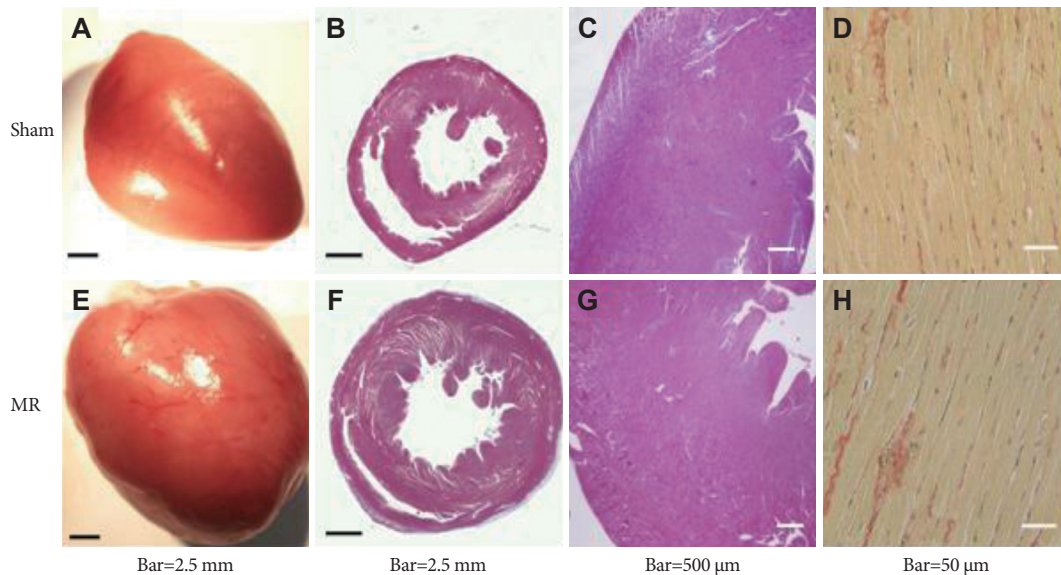


Fig. 6. Comparison of pathological results. Eccentric hypertrophy developed (E) and left ventricular mass increased (F). Masson's trichrome staining showed no significant difference in interstitial fibrosis (B, F, C and G). Picosirius red staining showed similar collagen content in both groups (D and H).

reference for future research and enhance our understanding of the pathophysiology and the development of new therapeutics for MR. Compared to large animal models,⁸⁾¹⁹⁾²⁰⁾ which have been used for MR experiments, this model has several advantages. First, LV remodeling and hemodynamic changes can be followed up in a shorter period of time, and survival analysis can be performed. Additionally, the costs are much lower; thus, the experiment is more feasible.

In their pioneering work, Pu et al.¹⁰⁾²¹⁾ developed an MR rat model for the first time. However, their report lacked details about the animal model, LV remodeling, exercise capacity, and histological findings that are critically important for future research. In the present study, we established a reliable small animal model of chronic MR using rats and verified the pathophysiological features of this model using serial echocardiography, PV analyses, an exercise test, and immunohistochemistry. We focused on several aspects to make the model useful for future experiments. Our first concern was that heart size and gender have been neglected in some previous experiments. In our pilot study, we found that rats showed rapid growth of the heart between 8 and 10 weeks of age (LV-ESD, 3.40 ± 0.15 mm vs. 4.02 ± 0.27 mm; LVEDD, 6.41 ± 0.34 mm vs. 7.31 ± 0.34 mm for 8 vs. 10 weeks of age, $p < 0.01$); thus, this period was not optimal for evaluating LV remodeling. Therefore, in this study, we used only 10 week old male rats. Second, we determined an adequate severity of MR to induce substantial LV remodeling without excessive mortality during the acute phase. We found that a 23G needle with an external diameter of 0.5 mm was the best for this purpose. At the postmortem study, the mean area of the hole was 0.79 ± 0.34 mm². Obviously, a “learning curve” was noted in our experience. In our first pilot study, the MR operation was suc-

cessful in only three of nine (33%) rats. It took 4 months for a consistent MR formation technique to develop. Interestingly, the mitral leaflet hole spontaneously regressed in some of the animals in our pilot study. Thus, confirmation of MR by serial echocardiography and direct visualization of the hole at harvest time were important.

In our chronic MR animal model, we described the natural course of LV remodeling in detail, which is important for future research. The acute stage was defined from creation of MR to the 2nd week after MR. We observed slight increases in the LV diastolic dimension without change in the systolic dimension; thus, hyperdynamic LV systolic function. During this stage, LV wall thinning occurred as the LV began to dilate. Four rats died during the acute stage (12%, 4/34) due to pulmonary edema (lung weight/body weight, mg/g; 1.94 ± 0.34 in the sham group vs. 9.51 ± 0.57 mg/g for the acute MR group). A chronic compensated stage was defined from the 3rd week to around the 14th week. In this stage, LV diastolic and systolic volume increased constantly. Although LVEF remained in the normal range, it decreased significantly in the MR group from the 12th week. At the 14th week, load-independent contractile indices such as ESPVR, dp/dt_{max} -EDV, and PRSW were significantly lower in the MR group, whereas diastolic parameters such as EDPVR, $-dp/dt$, and tau were not different between the groups. Indeed, MR is one of the very few cardiac diseases in which diastolic function is supernormal.²²⁾²³⁾ Corin et al.²³⁾ showed that the chronic adaptation to volume overload in chronic MR tends to decrease LV chamber stiffness. They demonstrated that elevated absolute and normalized diastolic filling rates and increased absolute dimension lengthening are found in chronic MR irrespective of systolic function. Additionally, we did not find

any changes in the LV collagen fraction or fibrosis in this stage of MR. However, the differing results regarding the effects of volume overload on collagen turnover may be due to species differences, the severity of volume overload, and the examination stage²⁴⁻²⁶ and need to be further investigated. Decomensation seemed to begin after the 14th week and became evident between the 20th and 26th week when mortality increased dramatically.

Study limitations

The development of miniaturized conductance catheters has enabled evaluation in the PV plane and allowed quantification of LV volumes and load-independent indices of contractility.^{27,28} However, because of methodological limitations, calibration of the volume signal remains challenging. Two approaches are generally taken with regards to the actual calibration procedure. One is cuvette calibration, while the other is an aortic flow calibration. However, in our experience, the cuvette method may yield inaccurate values, as the cylinders do not reflect the current distribution in the rat heart. The aortic flow measurement would underestimate LV volumes because of the MR. Therefore, in the present study, true volumes were calculated with a correction based on the LV EF using echocardiography and a saline calibration for Vo. The last echocardiography was performed just before the chest was opened at the 14th week after MR. An echocardiographic examination was performed with isoflurane anesthesia to maintain the same physiological conditions.

Conclusion

We established a small animal chronic MR model and verified the pathophysiological features of this model using serial echocardiography, a treadmill test, PV analyses, and a survival analysis. This model may provide a useful tool for future research in MR and volume overload heart failure.

Acknowledgments

This study was supported by a grant from the Korea Institute of Medicine and the Korea Healthcare Technology R&D Project, Ministry for Health, Welfare, and Family Affairs, Republic of Korea (A090458 and A080659).

The authors are grateful to Miss Hye-Won Lee and Ha-Na Kim for technical assistance.

REFERENCES

- Eriksson H. *Heart failure: a growing public health problem. J Intern Med* 1995;237:135-41.
- Mosterd A, Hoes AW. *Clinical epidemiology of heart failure. Heart* 2007;93:1137-46.
- Patten RD, Hall-Porter MR. *Small animal models of heart failure: development of novel therapies, past and present. Circ Heart Fail* 2009;2:138-44.
- Monnet E, Chachques JC. *Animal models of heart failure: what is new? Ann Thorac Surg* 2005;79:1445-53.
- Pacher P, Nagayama T, Mukhopadhyay P, B atkai S, Kass DA. *Measurement of cardiac function using pressure-volume conductance catheter technique in mice and rats. Nat Protoc* 2008;3:1422-34.
- Singh JP, Evans JC, Levy D, et al. *Prevalence and clinical determinants of mitral, tricuspid, and aortic regurgitation (the Framingham Heart Study). Am J Cardiol* 1999;83:897-902, Erratum in: *Am J Cardiol* 1999;84:1143.
- Nkomo VT, Gardin JM, Skelton TN, Gottdiener JJ, Scott CG, Enriquez-Sarano M. *Burden of valvular heart diseases: a population-based study. Lancet* 2006;368:1005-11.
- Zheng J, Chen Y, Pat B, et al. *Microarray identifies extensive down-regulation of noncollagen extracellular matrix and profibrotic growth factor genes in chronic isolated mitral regurgitation in the dog. Circulation* 2009;119:2086-95.
- Mishra YK, Mittal S, Jaguri P, Trehan N. *Coapsys mitral annuloplasty for chronic functional ischemic mitral regurgitation: 1-year results. Ann Thorac Surg* 2006;81:42-6.
- Pu M, Gao Z, Li J, Sinoway L, Davidson WR Jr. *Development of a new animal model of chronic mitral regurgitation in rats under transesophageal echocardiographic guidance. J Am Soc Echocardiogr* 2005;18:468-74.
- Reffelmann T, Kloner RA. *Trans-thoracic echocardiography in rats: evaluation of commonly used indices of left ventricular dimensions, contractile performance, and hypertrophy in a genetic model of hypertrophic heart failure (SHHF-Mcc-facp-Rats) in comparison with Wistar rats during aging. Basic Res Cardiol* 2003;98:275-84.
- Litwin SE, Katz SE, Weinberg EO, Lorell BH, Aurigemma GP, Douglas PS. *Serial echocardiographic-Doppler assessment of left ventricular geometry and function in rats with pressure-overload hypertrophy: chronic angiotensin-converting enzyme inhibition attenuates the transition to heart failure. Circulation*. 1995;91:2642-54.
- Helmcke F, Nanda NC, Hsiung MC, et al. *Color Doppler assessment of mitral regurgitation with orthogonal planes. Circulation* 1987;75:175-83.
- Chang SA, Kim YJ, Lee HW, et al. *Effect of rosuvastatin on cardiac remodeling, function, and progression to heart failure in hypertensive heart with established left ventricular hypertrophy. Hypertension* 2009;54:591-7.
- Lips DJ, van der Nagel T, Steendijk P, et al. *Left ventricular pressure-volume measurements in mice: comparison of closed-chest versus open-chest approach. Basic Res Cardiol* 2004;99:351-9.
- Burkhoff D, Mirsky I, Suga H. *Assessment of systolic and diastolic ventricular properties via pressure-volume analysis: a guide for clinical, translational, and basic researchers. American J Physiol Heart Circ Physiol* 2005;289:H501-12.
- Ichihara S, Senbonmatsu T, Price E Jr, Ichiki T, Gaffney FA, Inagami T. *Angiotensin II type 2 receptor is essential for left ventricular hypertrophy and cardiac fibrosis in chronic angiotensin II-induced hypertension. Circulation* 2001;104:346-51.
- Monnet E, Chachques JC. *Animal models of heart failure: What is new? Ann Thorac Surg* 2005;79:1445-53.
- Daimon M, Shiota T, Gillinov AM, et al. *Percutaneous mitral valve repair for chronic ischemic mitral regurgitation: a real-time three-dimensional echocardiographic study in an ovine model. Circulation* 2005;111:2183-9.
- Chaput M, Handschumacher MD, Guerrero JL, et al. *Mitral leaflet adaptation to ventricular remodeling: prospective changes in a model of ischemic mitral regurgitation. Circulation* 2009;120(11 Suppl):S99-103.
- Pu M, Gao Z, Zhang X, et al. *Impact of mitral regurgitation on left ventricular anatomic and molecular remodeling and systolic function: implication for outcome. Am J Physiol Heart Circ Physiol* 2009;296:H1727-37.
- Zile MR, Tomita M, Nakano K, et al. *Effects of left ventricular volume overload produced by mitral regurgitation on diastolic function. Am J Physiol* 1991;261:H1471-80.
- Corin WJ, Murakami T, Monrad ES, Hess OM, Krayenbuehl HP. *Left ventricular passive diastolic properties in chronic mitral regurgitation. Circulation* 1991;83:797-807.
- Ryan TD, Rothstein EC, Aban I, et al. *Left ventricular eccentric re-*

- modeling and matrix loss are mediated by bradykinin and precede cardiomyocyte elongation in rats with volume overload. J Am Coll Cardiol 2007;49:811-21.*
- 25) Weber KT, Pick R, Silver MA, et al. *Fibrillar collagen and remodeling of dilated canine left ventricle. Circulation 1990;82:1387-401.*
- 26) Michel JB, Salzmann JL, Ossono Nlom M, Bruneval P, Barres D, Camilleri JP. *Morphometric analysis of collagen network and plasma perfused capillary bed in the myocardium of rats during evolution of cardiac hypertrophy. Basic Res Cardiol 1986;81:142-54.*
- 27) Pacher P, Mabley JG, Liaudet L, et al. *Left ventricular pressure-volume relationship in a rat model of advanced aging-associated heart failure. Am J Physiol Heart Circ Physiol 2004;287:H2132-7.*
- 28) Bátkai S, Pacher P, Osei-Hyiaman D, et al. *Endocannabinoids acting at cannabinoid-1 receptors regulate cardiovascular function in hypertension. Circulation 2004;110:1996-2002.*